Available online at www.sciencedirect.com

SciVerse ScienceDirect

Advances in Space Research 49 (2012) 1363–1372

ADVANCES IN SPACE RESEARCH (a COSPAR publication)

www.elsevier.com/locate/asr

Using GPS-SCINDA observations to study the correlation between scintillation, total electron content enhancement and depletions over the Kenyan region

J.O. Olwendo [a,d,*], P.J. Cilliers [b,1], P. Baki [c,2], C. Mito [d,3]

[a] Pwani University College, P.O. Box 195, 80108 Kilifi, Kenya
[b] South African National Space Agency, P.O. Box 32, Hermanus, South Africa
[c] Kenya Polytechnic University College, P.O. Box 52428, 00200 Nairobi, Kenya
[d] Department of Physics, University of Nairobi, P.O. Box 30197, 00100 Nairobi, Kenya

Received 23 August 2011; received in revised form 3 February 2012; accepted 4 February 2012
Available online 15 February 2012

Abstract

This paper presents the first results of total electron content (TEC) depletions and enhancement associated with ionospheric irregularities in the low latitude region over Kenya. At the low latitude ionosphere the diurnal behavior of scintillation is driven by the formation of large scale equatorial depletions which are formed by post-sunset plasma instabilities via the Rayleigh–Taylor instability near the magnetic equator. Data from the GPS scintillation receiver (GPS-SCINDA) located at the University of Nairobi (36.8°E, 1.27°S) for March 2011 was used in this study. The TEC depletions have been detected from satellite passes along the line of sight of the signal and the detected depletions have good correspondence with the occurrence of scintillation patches. TEC enhancement has been observed and is not correlated with increases in S_4 index and consecutive enhancements and depletions in TEC have also been observed which results into scintillation patches related to TEC depletions. The TEC depletions have been interpreted as plasma irregularities and inhomogeneities in the F region caused by plasma instabilities, while TEC enhancement have been interpreted as the manifestation of plasma density enhancements mainly associated with the equatorial ionization anomaly crest over this region. Occurrence of scintillation does happen at and around the ionization anomaly crest over Kenyan region. The presence of high ambient electron densities and large electron density gradients associated with small scale irregularities in the ionization anomaly regions have been linked to the occurrence of scintillation.

Keywords: Ionization anomaly crest; Ionospheric irregularities; Scintillation; TEC enhancement; TEC depletions

1. Introduction

Plasma depletions are the irregularities of the largest scale sizes that are associated with the equatorial spread F where the plasma density may be lowered by up to three orders of magnitude compared to the background plasma density [Heelis, 2004; Dashora and Pandey, 2005]. In the equatorial region during daytime the dynamo electric fields that are generated in the equatorial E region by thermospheric winds are normally transmitted along the magnetic field lines to the F-region altitudes. The dynamo electric fields which are normally eastward during the daytime causes an upward E × B plasma drift. The plasma that is lifted during the daytime then diffuses down the magnetic field lines and away from the equator due to the action of gravity. This results into the formation of ionization

* Corresponding author. Address: Pwani University College, P.O. Box 195, 80108 Kilifi, Kenya. Tel.: +254 720990555; fax: +254 417522128.
E-mail addresses: castrajoseph@yahoo.com (J.O. Olwendo), pjcilliers@sansa.org.za (P.J. Cilliers), paul.baki@gmail.com (P. Baki), collins@uonbi.ac.ke (C. Mito).
[1] Tel.: +27 283121196; fax: +27 283122039.
[2] Tel.: +254 343672; fax: +254 2219689.
[3] Tel.: +254 4442016; fax: +254 4442018.

0273-1177/$36.00
doi:10.1016/j.asr.2012.02.006

peaks in the subtropics on both sides of magnetic equator a feature commonly known as the equatorial anomaly (Hargreaves, 1992; Basu et al., 1999). Towards dusk, as the ionosphere co-rotates with the earth, the eastward component of the neutral wind increases with the wind blowing predominantly across the terminator from the dayside to the night side. The increased eastward wind component in combination with the sharp day-night conductivity gradients across the terminator leads to the pre-reversal enhancement in the eastward electric field (Rishbeth, 2000). The F layer therefore rises as the ionosphere co-rotates into darkness. Because of the absence of sunlight the electron density in the lower ionosphere rapidly decays and a steep vertical density gradient develops on the bottom side of the raised F layer. A density perturbation under certain conditions can trigger the Rayleigh–Taylor (R-T) instability on the bottom side of the F-layer. Once the instability is triggered, density irregularities develop and field aligned depletions then bubble up through the F layer (Schunk and Nagy, 2009).

Ionospheric density irregularities are a major impediment to radio wave communication as they result in scattering of the incident radio waves. This leads to rapid fluctuations of the phase and amplitude of transionospheric radio frequency signals. This phenomenon is the so called ionospheric scintillation (Dashora and Pandey, 2005). The degree to which the ionospheric irregularities produce scintillations is determined by the frequency of the signal compared to the plasma frequency and the strength of the irregularities (Kintner et al., 2007). Studies in the equatorial and low latitude zone using GPS satellites have revealed the occurrence of the VHF scintillation and fluctuations in the total electron content (TEC) (Dandekar and Groves, 2004). Since the TEC values are known to be highest around $\pm 15°$) magnetic latitudes (more commonly known as the Appleton anomaly or the equatorial ionization anomaly region), any fluctuations in the TEC at these latitudes would result in severe scintillation causing signal degradation. The data used for this study is from Nairobi, located near the crest of the equatorial ionization anomaly and therefore well situated for the measurement of TEC and Ionospheric scintillation. This has been the motivation for the initiation of ionospheric measurement equipment (GPS-SCINDA System) by Boston College in collaboration with the Air Force Research Laboratory (AFRL) over Kenya for such studies. In this work we present a study on the correlation on the TEC depletions and scintillation events associated with the equatorial region for the month of March 2011.

2. Data and analysis

Ionospheric scintillation is characterized by rapid fluctuations in the amplitude and phase of trans-ionospheric radio signals due to variations in the local index of refraction along the propagation path. GPS-SCINDA software measures the intensity of amplitude scintillation given by the scintillation intensity index S_4 as (Carrano, 2007);

$$S_4 = \frac{\sqrt{\langle I^2 \rangle - \langle I \rangle^2}}{\langle I \rangle} \tag{1}$$

where I represents the signal intensity (amplitude squared). The ionosphere imparts a group delay and carrier phase advances to a radio signal. To a first order the group delay and phase advance are equal in magnitude, opposite in sign and proportional to the total electron content (TEC)

$$\Delta t = 40.30 \frac{TEC}{cf^2} \tag{2}$$

where f is the frequency of the signal in Hz and c is the speed of light in m/s. The slant TEC is the number of electrons in a column of 1 m^2 cross section centered on the ray path, from the GPS satellite to the GPS receiver on the ground. The TEC is measured in TEC units where 1 TEC unit is equal to 10^{16} electrons per m^2.

The GPS-SCINDA software computes relative TEC (TEC_R) as well as the differential pseudo-range and differential phase among other ionospheric statistics that can be used to obtain a more accurate TEC in post-processing. The relative TEC measurement computed by SCINDA software are based on 60 s averages of the differential pseudo-ranges (DPR) and differential carrier phase (DCP). The DPR is leveled to the DCP using all the data for each continuous phase arc.

$$TEC_R = DCP + \langle DPR - DCP \rangle_{ARC} \tag{3}$$

Once the relative TEC has been processed the calibrated TEC is obtained by subtraction of the satellite B_S and receiver B_R differential code biases from the relative TEC as;

$$TEC = TEC_R - A(B_R - B_S) \tag{4}$$

where A is a constant whose value is 2.854 TECU/ns. Using the single layer approximation for the ionosphere the calibrated slant TEC is converted to vertical TEC as follows;

$$TEC_V(B_R) = [TEC_R - A(B_R - B_S)]/M(\varepsilon, h) \tag{5}$$

where $M(\varepsilon, h)$ is the single layer mapping function of the ionosphere defined as

$$M(\varepsilon, h) = \sec\left\{\arcsin\left[\frac{R_e \cos\varepsilon}{R_e + h}\right]\right\} \tag{6}$$

where R_e is the Earth radius in km and ε is the elevation angle in radians. Here h is the ionospheric height which is assumed at 350 km.

For this particular study, the post processing of the relative TEC as illustrated from Eq. (4)–(6) was performed using the GPS TEC analysis application software developed by Seemala and Valladares (2008) of the Institute of Scientific Research, Boston College, USA. This software includes an algorithm for the estimation or downloading of the satellite and receiver biases. The biases free TEC (Vertical TEC) is written in ascii format together with other parameters defining the position of the satellite such as the time, elevation angle, azimuth angle, and the longitude and latitude of the Ionospheric Pierce Points (IPP).

3. Observations

The results presented here relate to March 2011 when geomagnetic quiet conditions prevailed. Thus the events discussed are mainly based on the regional ionospheric dynamics. Results obtained along the ray path from different satellite passes designated by the pseudorandom number (PRN) on different dates are shown in the following diagrams. In the diagrams presented each of the figures has three panels. The horizontal axis of each panel corresponds to the Universal Time (UT). The top panel of each figure gives the variation of the line of sight elevation angle in degrees and the amplitude scintillation intensity index (S_4). The second panel gives the variation of the line of sight total electron content (TEC) converted to vertical TEC by means of Eq. (5) and by averaging all the VTEC values for the visible satellites, the third panel depicts the geographic latitudes and geographic longitude of the IPP, computed from the elevation and azimuth angles of the satellite at each instant as seen from Nairobi station. Since at low elevation angles the received signal may suffer from multipath reflections we have only considered data for ray paths with elevation angles greater than 20° in our analysis.

TEC depletions consist of a rapid reduction in TEC value that lasts from 10 to 60 min followed by a gradual recovery to a level near the TEC value preceding the depletion (Dashora and Pandey, 2005). The TEC depletions that we are considering are produced by plasma bubbles drifting across the line-of-sight between the GPS receiver and the satellite. Such bubbles lead to ionospheric irregularities which are associated with intense scintillation on radio signals. Ionospheric irregularities develop in the evening hours at F-region altitudes where the depletions occur. Since the edges of the depletions are very sharp, they result in large time rate of change of TEC even during magnetically quiet conditions (DasGupta et al., 2007). Processes such as the nighttime decay of the F-layer and the density redistribution caused by the fountain effect also lessen the TEC values. However these processes result in gradual TEC decrease slopes and an absence of the recovery segment (Valladares et al., 2004). Changes in the slant length can also result in a slow variation of the TEC. Another type of plasma irregularity which has complimentary occurrence with plasma depletion is the plasma blob. A Plasma blob has been previously observed as a localized plasma density enhancement (Dashora and Pandey, 2005). Since the TEC is a measurement of the integral of plasma density, the enhancement in the plasma density can be observed as TEC enhancement using GPS observations (Yanhong et al., 2008).

3.1. Depletions in TEC

The general morphology of TEC depletions and their association with strong levels of VHF scintillation have been previously reported in the equatorial region (Aarons et al., 1994, Basu et al., 1999; de Paula et al., 2003). Similar correlations in the occurrences of bubbles and scintillation have been noted in this study.

Fig. 1 through 4 gives the results for different satellites on different days when significant scintillation events were recorded. While using the GPS-SCINDA system to measure amplitude scintillation, we identify scintillation events at scintillation index greater than 0.3. In Figs. 1–4, S_4 index levels greater than 0.3 have been marked with a red asterisk as an indication of geophysical phenomenon arising from ionospheric scintillation. At lower elevation angles (<20°) the scintillation index is prone to errors mainly arising from superimposed multipath effects on satellite signals which inflate scintillation index values and falsely indicate ionospheric scintillation activity. In the analysis of TEC depletions we have ignored results associated with low elevation angles less than 20°.

Fig. 1 gives the results relating to satellite PRN 26 on 30th March 2011.

With reference to Fig. 1, this satellite is observable from about 20° above the horizon and its highest elevation is about 60° with respect to the site of observation. The satellite goes below the horizon just after 21:00 UT. The variation of TEC is shown in the second panel of Fig. 1. Four depletions are detected from the satellite pass, and these depletions have good correspondence with occurrence of scintillation patches. The reduction in TEC has been identified as plasma depletion where TEC values decrease significantly. As seen in panel 1 in Fig. 1, the S_4 index is at its minimum noise level prior to the appearance of the depletion in TEC. It suddenly shoots to a value greater than the threshold of 0.3 coinciding with the occurrence of the TEC depletion. For the observed depletion the IPP latitude varies from 0° to 3°S, its longitude is however nearly constant around 36°E. The TEC values recover after the dip at 19:00 UT to a constant value thereafter up to about 20:30 UT when depletion in TEC occurs again.

Results obtained on 31st March, 2011 are presented in Fig. 2 for PRN 26. As is evident from Fig. 2, the satellite attains a very high elevation of about 60°. Three consecutive depletions in TEC are seen between 18:00 UT and 20:00 UT. The depletions that occurred just before 18:00 UT have been neglected since the satellite was at lower elevation of less than 20° where the scintillation results suffer from multipath errors which inflate their values. As evident from this fig., the appearance of TEC depletions (above 20° elevation) has been marked with arrows. Corresponding to TEC depletions are sudden increase in S_4 index to higher values of greater than 0.3 forming scintillation patches as seen in panel one.

It is observed that between sets of depletions, the variation in TEC is smooth and scintillation index is at lowest noise levels. We also note that scintillation do not occur continuously over a long interval of time, but in small patches with clear gaps in between. As observed from panel three in Fig. 2, the IPP geographic longitude between the times of appearance of the sets of depletions remains

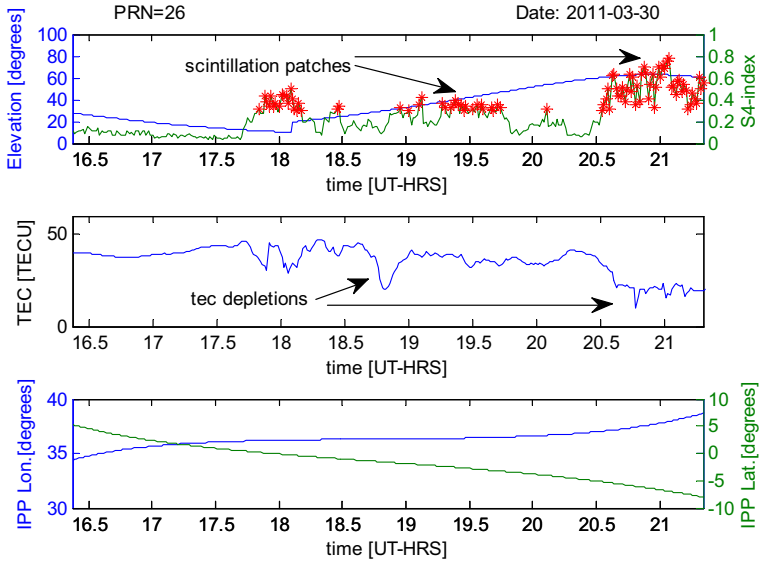

Fig. 1. Variation of TEC and S_4 index on 2011-03-30 relating to PRN 26. The top panel gives the S_4 index and satellite elevation angle. The second panel gives the variation of TEC and the third panel gives variation of IPP latitude and Longitude. The angle mask is set at 20 degrees.

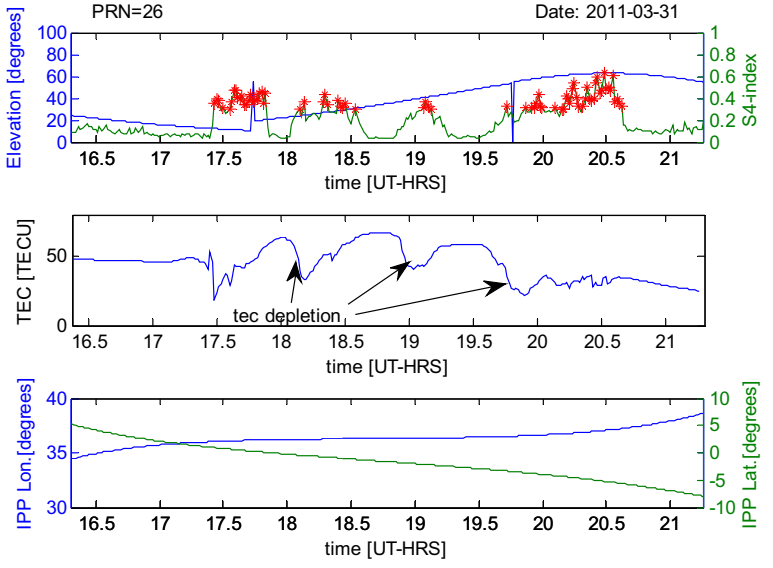

Fig. 2. Variation of TEC and S_4 index on 2011-03-31 relating to PRN 26.

constant and is about 36°E implying that the satellite is moving along the geographic meridian.

Results relating to PRN 10 observed on 9th March 2011 are given in Fig. 3.

After about 15:00 UT when the satellite was 30° above the horizon, the TEC values vary smoothly with constant decrease up to about 17:45 UT. Thereafter the TEC variation shows depletion. Unlike other observations when we saw well separated regions of depletions, in this case the depletion is single and extended as shown by the time spread of occurrence (between 17:45 and 18:30 UT). The TEC depletion in Fig. 3 is characterized by a depth larger than 24 TEC units. The wider and deeper depletion has a correspondence with strong levels of scintillation as seen from panel one on the same Fig. 4. The depletion detected has a sharp gradient and a depth of TEC which is more than 50% of the Total TEC before depletion started. The width of the depletion is 43 min and is associated with strong levels of scintillation that reach a maximum of $S_4 = 0.74$ when the elevation angle of the satellite is 30.5°. The most striking feature in Fig. 3 is the absence of scintillation where TEC variations are smooth.

3.2. Enhancement in TEC

Consecutive enhancement and depletions in TEC observed on 15th March 2011 along the ray paths from PRN 26 is shown in Fig. 4(a). The first consecutive depletions

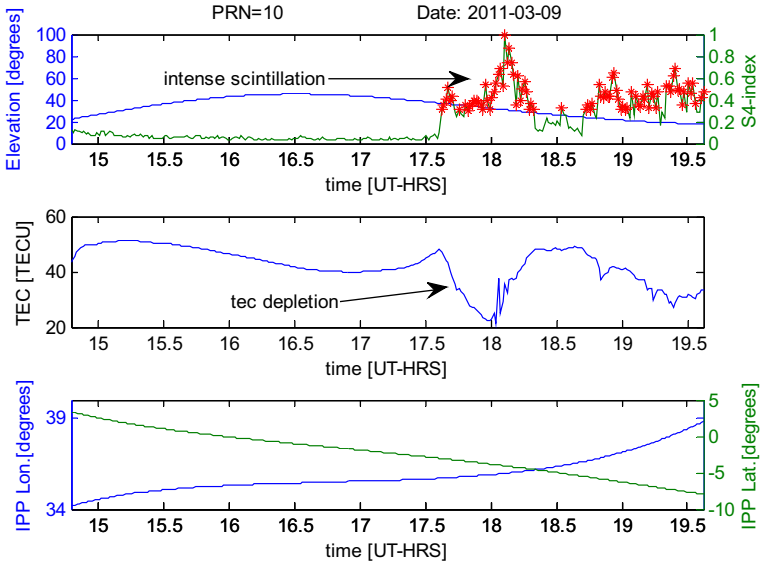

Fig. 3. Variation of TEC and S_4 index on 2011-03-09 relating to PRN 10.

and enhancements occur just before 19:00 UT. Fig. 4(a) shows that during the periods of consecutive TEC enhancement and TEC depletions, patches of scintillation are observed correlating to depletions while the S_4 index drops to the noise levels during enhancement. For all these features the longitude of the IPP was almost constant (36°E) and the latitude varied from 0° to 8°S.

The occurrence of scintillation and TEC enhancement without depletion has been studied further by using the data of day 14/03/2011 which was a quiet-day in the context that it did not have any scintillation observations. The TEC plot for the same is shown on Fig. 4(b). As seen from panel two of Fig. 4(b), at about 18:00 UT (21:00 LT) TEC values were at ~30 TECU. A gradual rise in TEC is observed reaching a maximum of ~50 TECU at 20:00 UT (23:00 LT) and later dropping to ~24 TECU at 22:00 UT. This observation does indicate that TEC enhancement during the satellite pass does not correlate with scintillation occurrences. It is also important to note that the TEC enhancement observed on 14th occurs more than 3 h after the sunset over this region. We thus relate this enhancement to satellite observation pass along the ionization anomaly crest where the background electron density does persist several hours after sunset. The temporal and spatial distribution of ionization post sunset is shown using TEC maps in Section 3.3.

We have noticed from Fig. 4(a) above that TEC depletions and TEC enhancement often occur consecutively. Fig. 5 shows a case where prior to TEC enhancement, there occurs a very steep gradient in TEC of ~20 TECU spanning over 30 min; this is then followed by abrupt TEC

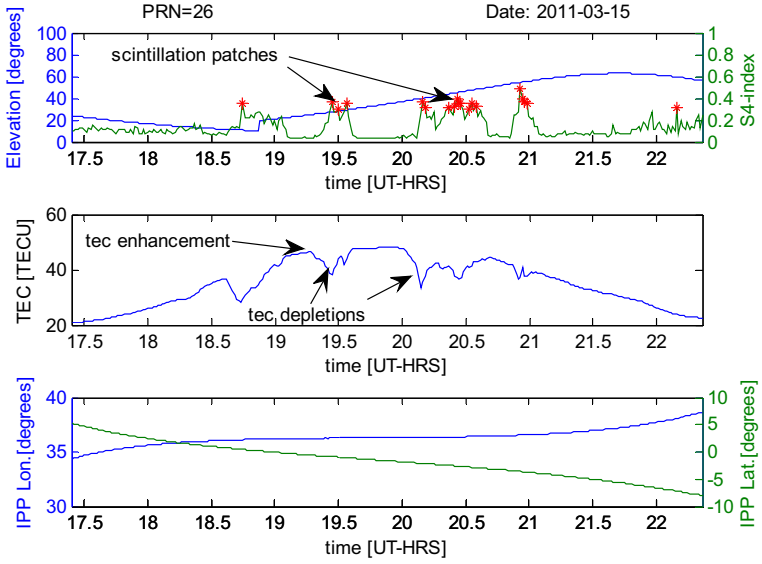

Fig. 4a. Observation of TEC enhancement around 19:00 UT on 15th March 2011 relating to PRN 26. The corresponding S_4 is very low when TEC enhancement occurs.

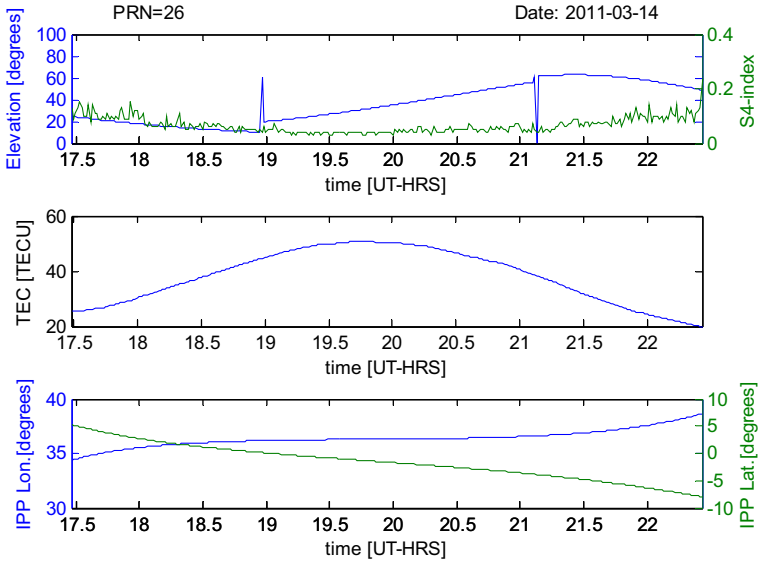

Fig. 4b. Observation of TEC on 14th March 2011 relating to PRN 26. The fig. shows that TEC values remain smooth on a quiet day (no scintillation day) and corresponding S_4 is maintained at the noise levels. Compared to Fig. 4(a) there was no TEC enhancement on quiet-day pass.

enhancement to levels prior to the drop. During depletions in TEC, intense scintillation are observed while the TEC increase is accompanied by a sudden drop in the scintillation as shown in panel two of Fig. 5. The duration of the enhancement is more than half an hour and the local time corresponding to this is about 20:30 LT with the geomagnetic latitude of the IPP at this time being about 0°. The enhancement is completely unrelated to the preceding increase in the S_4 index.

3.3. TEC Enhancement and scintillation morphology over the Kenyan region

The morphology of equatorial scintillation is characterized by the location of the largest ionospheric densities which are normally referred to as the equatorial ionization anomaly crests, about 15° from the magnetic equator. These crests are formed during the daytime when solar heating of the thermosphere drives an eastward dynamo electric field. The electric field drives an upward flux of ionization at the equator, which subsequently falls down magnetic field lines increasing ionization density in two bands called the equatorial anomalies.

Since Kenyan region is within the anomaly crests, the morphology of this anomaly crests would be vital for the understanding of TEC enhancement mechanism associated with observation in Figs. 1–5. In this regard we have developed regional TEC maps for the Kenyan region using four International GNSS Services (IGS) stations namely; rcmn, moiu, mal2 all within Kenya, and to cover the

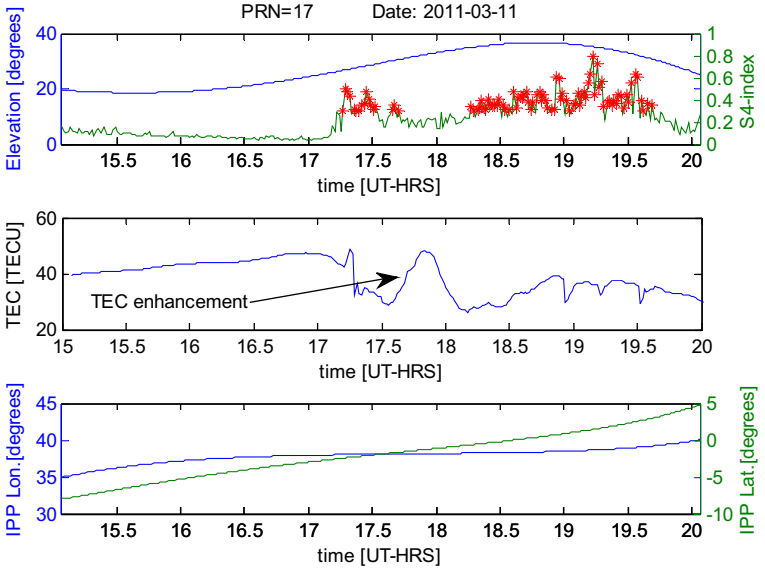

Fig. 5. Observation of TEC enhancement prior to 18:00 UT on 11th March 2011 related to PRN 17. The corresponding S_4 is very low when TEC enhancement occurs and unlike in previous observation the TEC enhancement is isolated from depletions. .

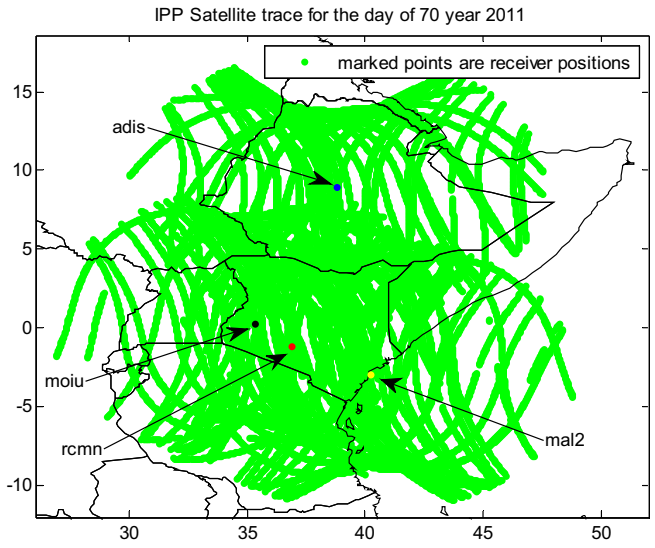

Fig. 6. IPP coverage over the Kenyan region on day 70 of 2011.

TEC distribution in the northern part we have used the adis station located in Ethiopia. The IPP trace of satellite coverage over the Kenyan region from the mentioned IGS receiver stations is shown in Fig. 6 below.

The regional TEC maps developed for this study are created by interpolation and extrapolation of TEC observation from the said stations over the Kenyan region using the ASHA algorithm described in Eq. (7). The ASHA algorithm calculates TEC at any latitude or longitude from dual frequency GPS observations using a spherical harmonic expansion according to the following mathematical expression (Opperman et al., 2007);

$$TEC(\lambda,\phi)=\sum_{n=0}^{N}\sum_{m=0}^{n}\overline{P_{nm}}\cos(\phi)[a_{nm}\sin(m\lambda)+b_{nm}\cos(m\lambda)] \quad (7)$$

where λ is the sun-fixed longitude, ϕ is the co-latitude, P_{nm} are the normalized associated Legendre functions, a_{nm} and b_{nm} are the spherical harmonic coefficients estimated from a weighted least squares solution, n and m are the degree and order of the spherical expansion respectively. In the ASHA model, the Differential Clock Biases (DCBs), from both satellite transmitters and GPS receivers are estimated along with the spherical harmonic coefficients using the least squares method. For detailed discussions about the ASHA model, the reader is referred to Opperman et al. (2007) and Opperman (2007). Fig. 7 gives the TEC map over the Kenyan region for the 11th of March, 2011. This was the day when a steep TEC gradients and TEC enhancement was observed from PRN 17.

The TEC maps in Fig. 7, show that the TEC peaks around 12:00 UT (15:00 LT). At about 14:00 UT the TEC starts decreasing since this time is the start of sunset over this region. At about 18:00 UT (21:00 LT) there is still an enhancement in TEC in the southern region. Since this time corresponds to about three hours after sunset, we associate the TEC enhancement remaining at this time to be associated with the southern equatorial anomaly crest. We relate the TEC peaks to the TEC enhancement observed on PRN 17 in Fig. 5. To show this we plot the IPP trace for PRN 17 for this particular day with color coding according to TEC in Fig. 8.

The scenario presented in Figs. 7 and 8 suggest that the largest scintillation events are strongly correlated with the

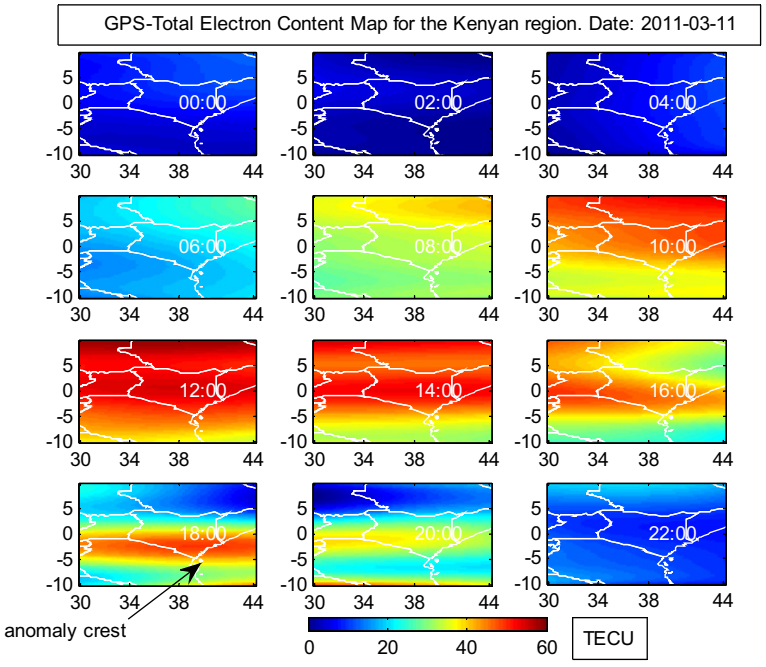

Fig. 7. TEC maps in two hour increments over the Kenyan region interpolated from a 12 degree ASHA solution on a 0.25 × 0.25° grid. The times indicated on the maps are in UT.

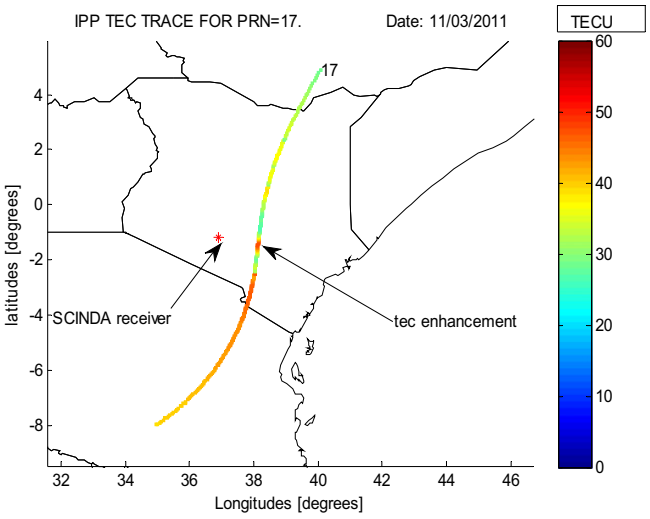

Fig. 8. IPP TEC trace observed at NAIROBI SCINDA station between 15:00-20:00 UT for PRN 17 on 11th March, 2011.

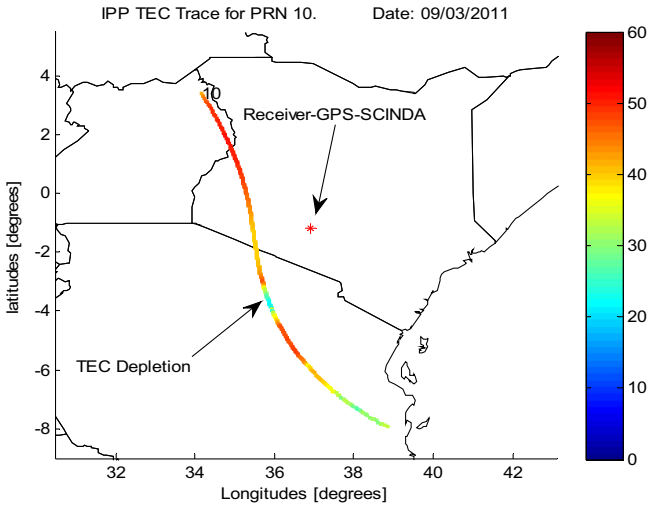

Fig. 10. IPP TEC trace observed at NAIROBI SCINDA station between 15:00 and 20:00 UT for PRN 10 on 09th March, 2011.

regions of increased background electron density and where steep gradients in TEC are found as shown in Fig. 5. From Figs. 7 and 8 scintillation appears close to the edges of the enhanced ionization anomaly crests. Near the anomaly crest region, because of increased electron densities and the presence of large gradient, the generation of small scale irregularities is relatively high which contribute to the occurrence of strong scintillations (Ray et al., 2006). Fig. 9 and 10 further illustrates the occurrence of scintillation at and around the anomaly crest if steep TEC gradients occur. The Figs. 9 and 10 corresponds to observation related to scintillation observation in Fig. 3 where we noticed a very steep gradient in TEC. The steep gradients as shown in Fig. 9 are at the edges of the ionization anomaly.

4. Discussion and conclusion

GPS scintillation at low latitude are primarily associated with Equatorial Spread F. Equatorial Spread F is caused by ionospheric irregularities with spatial range extending from 100 km to less than 1 m (Kintner et al., 2007). Equatorial Spread F develops shortly after sunset and propagates both upward and to off equatorial latitudes in the electromagnetic equivalent of the Rayleigh–Taylor instability (Michael, 2009). As the lower density ionosphere moves upward into the higher density ionosphere, it creates a 'hole' sometimes called a bubble. After the hole develops and rises to the topside F region ionosphere, it typically stops evolving and the structure is 'frozen' into the moving

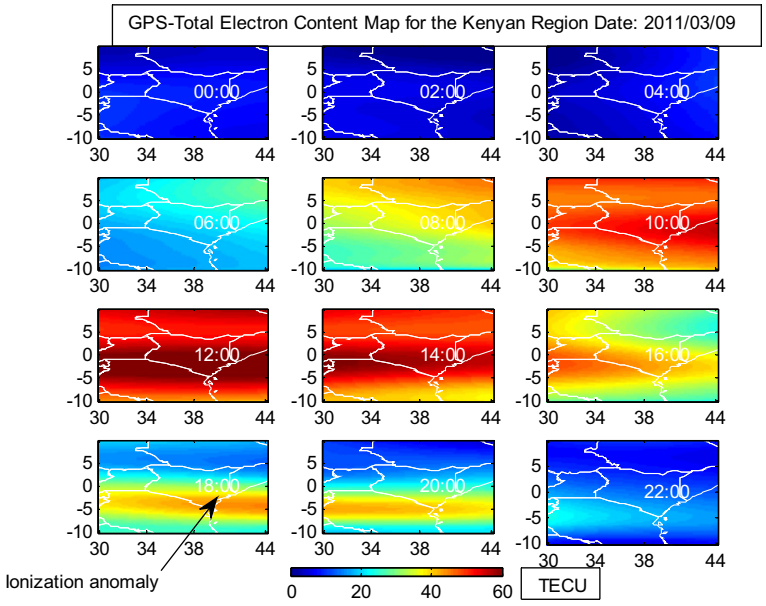

Fig. 9. TEC maps in two hour increments over the Kenyan region interpolated from a 12 degree ASHA solution on a 0.25 × 0.25° grid. The times indicated on the maps are in UT.

ionosphere. These frozen structures in the moving ionosphere are what contribute to the observed ionospheric irregularities commonly called the plasma bubbles.

Since the F region electron density heavily weighs the TEC, and TEC being a measurement of the integral plasma density, any variation therefore in the F-region plasma density is likely to be reflected in the TEC. Sudden reductions in TEC observed in the nighttime low-latitude F region have been identified with the plasma density depletion of equatorial origin (Dashora and Pandey, 2005, Theodore and Kintner, 1999, Basu et al., 1999). Consistent with this definition, the reduction in the TEC reported in Fig. 1 through 4 have been identified as a manifestation of the plasma density depletions of equatorial origin. Associated with these depletions are the smaller scale plasma density irregularities which manifest as increase in scintillation intensity index (S_4) when they are located along the signal path. This is the reason for the observations in the increases in S_4 index at the same time when the depletion in TEC are observed. We thus conclude that over this region which is located near the equatorial ionization anomaly crest, the relation between amplitude scintillations and depletions in TEC is one-to-one. Using the IPP latitudes and longitudes we have also seen that the depletions in TEC are field aligned (geographic meridian coincides with the magnetic at the Kenyan region) and this confirms their equatorial origin.

The ExB drifts and gravitational field-aligned flows create sharp density gradients on the poleward boundaries of the bubbles. As a consequence of the expansions (resurgence) of the fountain effect the ionosphere at latitudes of the anomaly crests exhibits remarkable spartial gradients of TEC (Raghavarao et al., 1988). As the well developed large-scale bubbles structures extend along the magnetic field lines their intersection with regions of increased background electron density and steepest density gradients may set up, at the wall of the bubbles, secondary instability processes that create conditions favorable for the generation of small scale plasma irregularities (Ray et al., 2006; Muella et al., 2010). This argument confirms our observation as shown in Figs. 1 and 5, and also the occurrence of anomaly and scintillation as shown in Fig. 7 and 9.

In Fig. 5 we have observed very steep TEC gradients followed by large TEC enhancements. Unlike a similar observation made by Dashora and Pandey (2005), we have noticed a higher TEC increase of more than 15 TECU expanding over more than 30 minutes interval. The enhancement was completely devoid of an increase in S_4 index. Previous studies in night-time TEC enhancement at the equatorial anomaly region in China have indicated that TEC enhancement near the equator may be related to polarization electric fields associated with the depletions which generate localized regions of plasma enhancements (Yanhong et al., 2008). The station on which this study was done is located near the equatorial ionization anomaly crest. The anomaly crest are formed during the daytime by eastward dynamo electric field which drives an upward flux of ionization at the equator, which subsequently falls down magnetic field lines at more polar locations increasing the ionization density at the subtropics forming the anomaly crests. The enhanced ionization densities remain through darkness depending on the altitude and recombination rate. The observed TEC enhancement in Fig. 5 is associated with the southern anomaly crest since the satellite crossed the southern anomaly crest around 18:00 UT, a time coincident with the observation in TEC enhancement. Preceding the TEC enhancement between 18:30 UT and 19:30 UT, there was intense scintillation on the same satellite while still within the anomaly crest, this is shown in Fig. 5 panel one. We associate this to the equatorial bubbles initiated shortly after sunset which rise and form flux tubes which map to more poleward latitudes. And due to stirring motions associated with the bubbles turbulence they reach the anomaly crests, where they produce most intense density irregularity leading to amplitude scintillation. This study therefore reports of a new feature of the equatorial anomaly crest which shows the existence of increased scintillation amplitude in the anomaly crest though for just a single night observation.

Acknowledgement

We appreciate the Air Force Research Laboratory Collaboration and Boston College for the donation and maintenance of the SCINDA-GPS system at the University of Nairobi (Kenya) and Dr. Opperman, B.D.L. of the South African National Space Agency for his useful guidance in development of regional GPS TEC mapping software. The authors would also wish to thank the reviewers for their helpful comments and suggestions on the paper.

References

Aarons, J., Mendillo, M., Kudeki, E., Yantosca, R. GPS phase fluctuations in the equatorial region during the MISETA 1994 campaign. J. Geophys. Res. 101 (A12), 26851–26862, 1994.

DasGupta, A., Paul, A., Das, A. Ionospheric total electron content (TEC) studies with GPS in the equatorial region. Indian J. Radio Space Phys. 36, 278–292, 2007.

Basu, S., Groves, K.M., Quinn, J.M., Doherty, P. A comparison of TEC fluctuations and Scintillation at Ascension Island. J. Atmos. Terr. Phys. 61, 1219–1226, 1999.

Carrano, Charles S. GPS-SCINDA: A real-time GPS Data Acquisition And Ionospheric Analysis System For Scinda. Atmospheric and Environmental Research, Inc., GPS-SCINDA, 2007.

Dandekar, B.S., Groves, K.M. Using ionospheric scintillation observation for studying the morphology of equatorial ionosphere bubbles. Radio Sci. 39, RS3010, doi:10.1029/2003RS003020, 2004.

Dashora, N., Pandey, R. Observations in equatorial anomaly region of total electron content enhancements and depletions. Ann. Geophys. 23, 2449–2456, 2005.

De Paula, E.R., Rodrigues, F.S., Iyer, K.N., Kantor, I.J., Abdu, M.A., Kintner, P.M., Ledvina, B.M., Kil, H. Equatorial anomaly effects on GPS scintillations in Brazil. Adv. Space Res. 31 (3), 749–754, 2003.

Hargreaves, J.K. The Solar-terrestrial Environment: An Introduction to Geospace – The Science of the Terrestrial Upper Atmosphere, Ionosphere and magnetosphere. Cambridge University Press, 1992.

Heelis, R.A. Electrodynamics in the low and middle latitude ionosphere, a tutorial. J. Atmos. Terr. Phys. 66, 825–838, 2004.

Kintner, P.M., Ledvina, B.M., de Paula, E.R. GPS and ionospheric scintillations. Space, Weather 5, S09003, doi:10.1029/2006SW000260, 2007.

Michael Kelley, C. 2009. The earth's ionosphere: plasma physics and electrodynamics, Int. Geophys. Ser. 96.

Muella, M.T.A.H., Kherani, E.A., de Paula, E.R., Cerruti, A.P., Kintner, P.M., Kantor, I.J., Mitchell, C.N., Batista, I.S., Abdu, M.A. Scintillation producing Fresnel-scale Irregularities associated with the regions of steepest TEC gradients adjacent to the Equatorial ionization anomaly. J. Geophys. Res. 115, A03301, doi:10.1029/2009JA014788, 2010.

Muella, M.T.A.H., Kherani, E.A., de Paula, E.R., Cerruti, A.P., Kintner, P.M., Kantor, I.J., Mitchell, C.N., Batista, I.S., Abdu, M.A. Scintillation producing Fresnel-scale Irregularities associated with the regions of steepest TEC gradients adjacent to the Equatorial ionization anomaly. J. Geophys. Res. 115, A03301, doi:10.1029/2009JA014788, 2007.

Opperman, B.D.L., Cilliers, P.J., McKinnell, L.A., Haggard, R. Development of a regional GPS-based Ionospheric TEC model for South Africa. Adv. Space Res. 39, 808–815, 2007.

Rishbeth, H. The equatorial F-layer progress and puzzles. Ann. Geophys. 18, 730–739 (Spring-Verlag), 2000.

Raghavarao, R., Nageswararao, M., Hanumath Sastri, J., Vyas, G.D., Sriramarao, M. Role of equatorial ionization anomaly in the initiation of equatorial spread F. J. Geophys. Res. 93 (A6), 5959–5964, 1988.

Schunk, R.W., Nagy, A.F. Ionospheres, Physics, Plasma Physics and Chemistry. Cambridge University Press, 2009.

Seemala, G.K., Valladares, C.E. Statistics of total electron content depletions observed over the South American continent for the year 2008. Radio Sci. 46, RS5019, doi:10.1029/2011RS004722, 2008.

Ray, S., Paul, A., DasGupta, A. Equatorial scintillations in relation to the development of ionization anomaly. Ann. Geophys. 24, 1429–1442, 2006.

Theodore, L. Beach, Kintner, Paul M. Simultaneous Global Positioning System observations of Equatorial scintillation and total electron content fluctuations. J. Geophys. Res. 104 (A10), 22553–22565, 1999.

Valladares, C.E., Villalobos, J., Sheehan, R., Hagan, M.P. Latitudinal extension of low- Latitude scintillation measured with a network of GPS receivers. Ann. Geophys. 22, 3155–3175, 2004.

Yanhong, Chen, Ma, Guanyi, Huang, Wengeng, Shen, Hua., Li, Jinghua Night-time total electron content enhancements at equatorial anomaly region in China. Adv. Space Res. 41, 617–623, 2008.